

# Estimation of reservoir quality from multi-attribute analysis by using a probabilistic neural network: case of Sarvak Formation in an offshore oil field

M. AKBARI<sup>1</sup> and M.A. RIAHI<sup>2</sup>

<sup>1</sup> *Department of Geology, Faculty of Sciences, Urmia University, Iran*

<sup>2</sup> *Institute of Geophysics, University of Tehran, Iran*

(Received: 24 August 2019; accepted: 4 May 2020)

**ABSTRACT** The objective of this research is to study the relationship between reservoir parameters and seismic attributes in order to determine the reservoir quality, estimate the porosity model, and plan for infill drilling in the oil field under study, based on seismic and well log data. Sarvak Formation in this oil field is characterised, using a combination of the seismic data, porosity logs, and seismic attributes. By estimating the porosity model through various methods including single-attribute regression, multi-attribute regression, and artificial neural network, the probabilistic neural network has shown to represent reliable results. Interpretation of data shows that the estimation of porosity model for the Sarvak Formation indicates high reservoir quality. Besides, comparing the porosity values, the well BS-06 has higher porosity than the well BS-01, which indicates that, the higher reservoir quality at the BS-06 well location. The obtained porosity model, showed that the highest porosity values are found around the seismic CDP location No. 30850. Therefore, this area can be considered for prospective infill drilling in the field development plans.

**Key words:** seismic data, porosity, neural network, Sarvak Formation, seismic attribute.

## 1. Introduction

The integration of well logging and seismic data has become increasingly important in recent years because of the shift from exploration to development of existing fields. Meanwhile, using core samples and well logs for development purposes provides the reservoir properties only at areas around and near the wells. Furthermore, determination of the correct porosity model of reservoir, from the petro-physical parameters, reduced financial and operational risks for drilling and completion. Using seismic data for estimating porosity as a petro-physical parameter can be helpful in making decisions for cases with high financial risk such as determining suitable drilling targets. A correct realisation of the porosity variations inside the gaseous sand will lead to mastering proper development plans for reservoir management. It is proved by rock physics principles that a relationship exists between the acoustic impedance and the porosity obtained from the petro-physical well logs. The use of impedance values obtained from the seismic inversion method for determining high and low porosity zones has been proposed by many researchers; it is evident that if the acoustic impedance is low, the porosity and the reservoir

potential is high (Dolberg *et al.*, 2000; Çemen *et al.*, 2014; McKie *et al.*, 2015). In this research, Model-Based Inversion (MBI) method has been used to estimate the acoustic-impedance model of the reservoir.

In addition to the acoustic impedance obtained from seismic inversion, which is considered as the external attribute, a series of other attributes, i.e. internal attributes, are derived from the seismic data in order to estimate the porosity along with using the acoustic impedance as an external attribute. In this study, in order to estimate a porosity model, three different methods have been used. These methods include single-attribute regression, multi-attribute regression, and the probabilistic neural network. It is known that the neural networks method offers superior results as compared to the multi-attribute regression and single-attribute methods (Hampson *et al.*, 2001; Russell, 2004).

Neural networks are able to detect similarities in the input, even though a particular input may have never been previously introduced to the network. This property allows for excellent interpolation capabilities, especially when the input data is noisy (Parsaeimaram *et al.*, 2013). Generally, the artificial neural network (ANN) methods are superior to the knowledge-based and rule-based expert systems since they have better generalisation and fault tolerance. The rationale for applying the neural network is that some part of the data is labelled as training data and is imported to a network firstly where the respective output data are already available. Therefore, the outputs are calculated by applying the learning algorithm on the network. The obtained outputs are compared with the optimum output of the network and the existing error between them is calculated and by the error distribution operations, the resulting error is distributed through the network parameters (i.e. weight and bias). By distributing the errors at each step, the network parameters are updated (Haykin, 1999). In order to properly train the network, in addition to the set of training data that are used, a series of data are introduced to the network for validation purposes. These data have not taken part in network training. Overfitting is a state in which the error for learning the network using training data decreases whereas the error for learning the network over the validation data increases. There are various algorithms of neural networks. In this research, three neural networks algorithms including Multilayer Feed-Forward Neural Network (MLFN), Probabilistic Neural Network (PNN), and Radial Basis Function Neural Network (RBFN) have been used for analysis and finally, in order to estimate porosity model, the PNN has been used.

Similar studies were performed in different regions. Leiphart and Hart (2001) used seismic attributes to estimate the reservoir properties in SE New Mexico. Basu and Verma (2013) used a similar approach to estimate the porosity in Cambay basin of India. Estimating the porosity model using MBI and PNN method was carried out by Al-Rahim and Hashem (2016) in an area located in southern Iraq and by Mahmood *et al.* (2017) in Balkassar area located in Pakistan, respectively. The results from a quantitative comparison carried out by Maurya and Singh (2019) in Alberta province of Canada indicated that PNN produces better statistical estimates for porosity distribution as compared to the multi-attribute regression. It also suggests that given seismic and well log data for a region, a combination of MBI and PNN can produce a more reliable estimate of the petrophysical properties.

The purpose of this research is to estimate the porosity distribution for the reservoir, based on seismic and well log data by using PNN, and plan for infill drilling in this oil field.

## 2. The geological setting of the studied area

The area of study is located in an offshore oil field, in Iran. The geographic location of some of the Persian Gulf hydrocarbon fields is shown in Fig. 1. The studied formation is the Sarvak Formation. This formation, as one of the formations inside the Bangestan group, is considered as one of the important stratigraphic units in the Zagros basin, due to its hydrocarbon potential. This formation deposited during the sea level rise of Late Aptian to Early Turonian and is characterised by limestone, dolomitic limestone, and clayey limestone. This formation consists of three parts: Lower (Madood), Middle (Ahmadi), and Upper Sarvak Formation (Omidvar *et al.*, 2015).

Since this formation is one of the most important reservoir horizons in many hydrocarbon fields of SW Iran, it has long been studied by the geologists. The Cenomanian-Thoronin period includes the formations of Mishrif, Ahmadi, and Ramilla (Saudi Arabia), Natieh (Oman), Durdar (south-eastern Turkey), Mishrif (Iraq) and Sarvak (Iran) (Omidvar *et al.*, 2015).

The upper boundary of the Sarvak Formation is discontinuous with part of Ilam Formation deposited on it where the lower boundary is transitional boundary with the Kazhdumi Formation (Fig. 2A). Lithology of these formations is mainly limestone and dolomite in some parts. Sarvak Formation includes two facies, shallow and deep. The lower part of the Sarvak Formation includes clay limestone, which is pelagic and the reservoir quality is lower as compared to the upper part of the formation (Taghavi *et al.*, 2006; Beiranvand *et al.*, 2007; Hajikazemi *et al.*, 2010; Rahimpour-Bonab *et al.*, 2012a). This formation is widely present in the Dezful embayment and the Persian Gulf. Many studies have focused on the Sarvak Formation, which, in a qualitative sense, has become known as the second biggest reservoir of Iran (Behdad *et al.*, 2010; Hajikazemi *et al.*, 2012; Rahimpour-Bonab *et al.*, 2012b). Fig. 2 shows the generalised chronostratigraphy

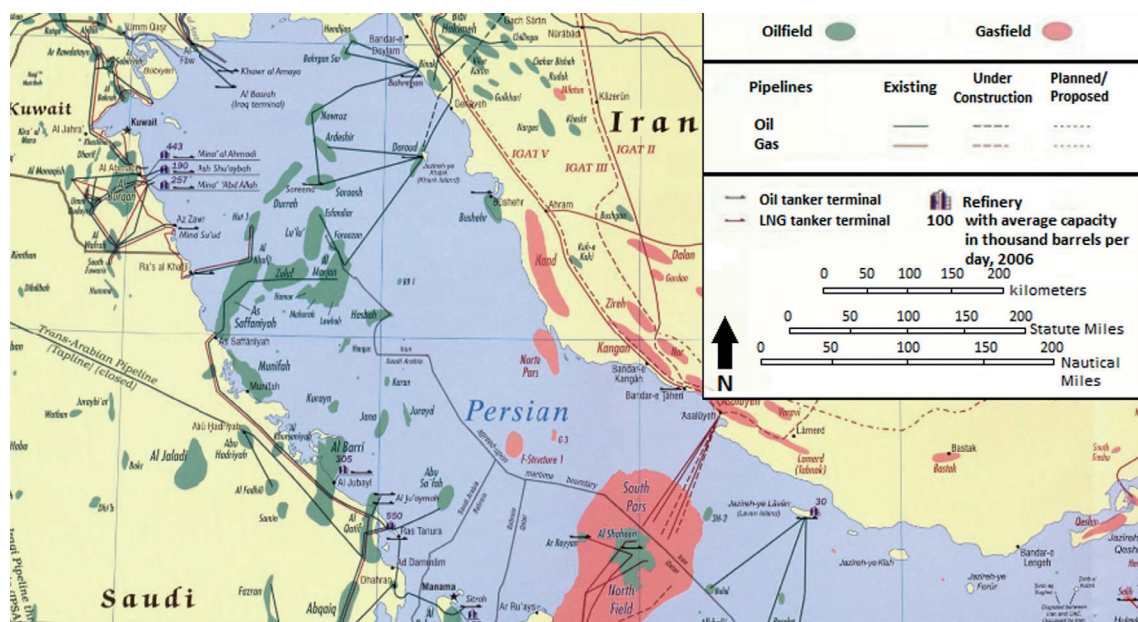


Fig. 1 - Geographic position of some hydrocarbon fields in the Persian Gulf (Central Intelligence Agency, 2001).

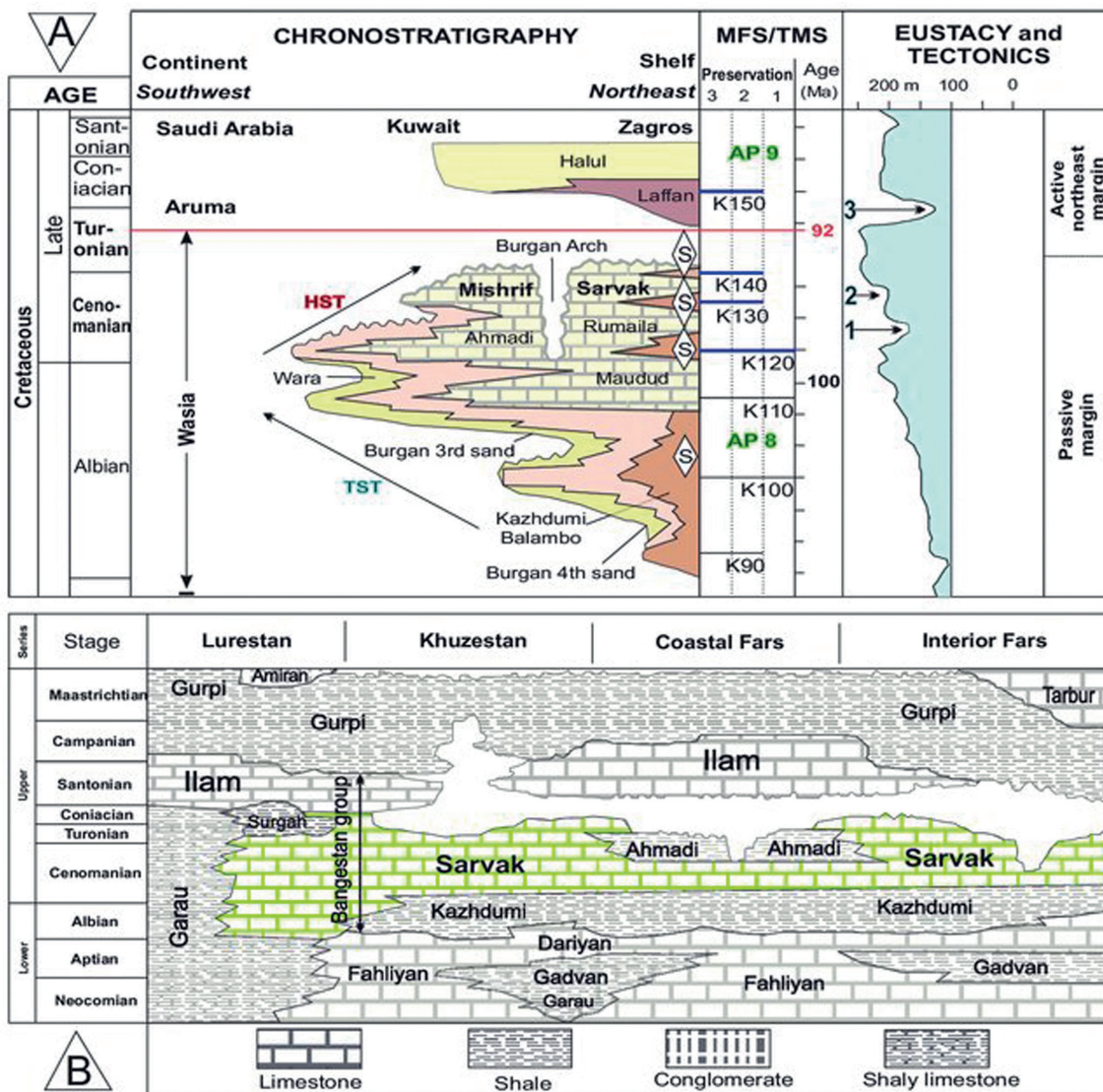


Fig. 2 - A) Generalised chronostratigraphy of the Cretaceous successions in the Zagros region (SW Iran), Kuwait, and Saudi Arabia together with eustasy and regional tectonics; B) detailed stratigraphy of the Cretaceous successions in different parts of Iran, including the Sarvak Formation of the Bangestan Group showing lateral facies and thickness variations (Rahimpour-Bonab *et al.*, 2012b).

of the Cretaceous successions in the Zagros region and detailed stratigraphy of the Cretaceous successions in different parts of Iran.

### 3. Data set and methods

#### 3.1. Data set

The “Persian Carpet 2000” or “PC-2000” seismic survey is the primary data set for this study which covers the entire Iranian part of the Persian Gulf with a dense grid of seismic lines and

provides the first seismic data for the Iranian part of the Oman Sea. The seismic grid was made up of  $2 \times 2$  km<sup>2</sup> line spacing oriented NW to SE and NE to SW.

The whole seismic data that are used in this research include three post-stack time migration (PSTM) two-dimension (2D) marine seismic lines with good quality, which is CDP sorted. Furthermore, the well-logging data from two drilling wells in this field, called BS-01 and BS-06, are used. These three seismic sections contained 9606 CDP gathers. One of these sections, where CDPs range from 30002 to 33064 (3062 CDP gathers), was selected for model-based seismic inversion, because it is located in the vicinity to both wells BS-01 and BS-06. The utilised petro-physical logs from wells BS-01 and BS-06 include density, porosity, and P-wave velocity. For the purpose of depth-time correction, the check-shot data from the two wells are also used.

The available data in this research were analysed by Hampson-Russell software (1999) (<https://iba.aapg.org/software/hampson-russell>). Four types of analyses are used by the Hampson-Russell software (1999) including: MBI, single-attribute analysis, multi-attribute analysis, and PNN analysis.

In this study, to perform model-based seismic inversion of seismic data, the STRATA module of the Hampson-Russell software (1999) was used. For such purpose, the seismic section, check shot data, density log, and P-wave velocity log are required.

In order to estimate the porosity model, the acoustic impedance section inverted from the seismic data and the available porosity well logs from the two drilled wells were used.

### *3.2. Methods developed in the Hampson-Russell software*

#### *3.2.1. Model-based inversion*

The MBI, also known as blocky inversion, is a post-stack inversion method, which computes the acoustic impedance from the seismic data sets. The method is based on the convolutional theory, which states that the seismic trace can be generated from the convolution of wavelet with the reflectivity function with addition of some noise (Maurya and Singh, 2019).

#### *3.2.2. Seismic attributes*

Seismic attributes are specific quantitative properties of seismic data and their applications are used since the 1970s. These attributes are considered as very useful tools for seismic data interpretation in mapping quantitative and qualitative geological properties, as each of these seismic attributes describe the physical or geological characteristics of the subsurface layers (Varasteh *et al.*, 2010).

Seismic attributes comprise information about seismic wave geometry, kinematics, dynamics, and statistical characteristics, which are derived from pre-stack or post-stack seismic data by mathematical transformations. In recent years, with the development of reservoir interpretation and seismic analysis requirements, many new attributes were extracted by conventional attributes. Seismic attributes have been successfully used for predicting reservoir lithology, estimation of hydrocarbon resources, and quantifying the reservoir properties (Rahimpour-Bonab, 2007; Li and Zhao, 2014).

#### *3.2.3. Multi-attribute linear regression*

Individual attributes may be representative for several possible events and the attempt to minimise this inherent uncertainty or non-uniqueness, should be done by combining multiple

attributes in a logical fashion. The multi-attribute linear regression uses hybrid attributes in order to estimate the porosity (Taner, 2001).

Step-wise regression is an efficient method to find the most prominent attributes for multi-attribute analysis. The step-wise regression consists of the following steps:

1. find the best attribute by an exhaustive search through the whole attributes, compute the prediction error for each attribute, and choose the attribute with the lowest error;
2. find the best pair of attributes from all combinations of the first attribute and other attributes. Again, the best pair is the pair that has the lowest prediction error;
3. find the best triplet, using the pair from step 2 and combining it with some other attribute;
4. continue the process as long as desired.

Step-wise regression therefore gives us a very efficient way of finding the best set of attributes, as they exhibit the lowest least squares error (Russell, 2004).

Step-wise regression will give a set of attributes that is guaranteed to reduce the total error as the number of attributes increases. The stopping criteria are based on the cross-validation technique in which a training sample is left out of procedure and it is predicted from the other samples. The error is, then, re-computed for the training sample that was left out. This procedure is repeated for the whole training samples and the error is averaged to give the total validation error. This computation is done as a function of the number of attributes, and the resulting graph usually shows an increase in validation error past some small number of attributes such as five or six (Russell, 2004).

#### 3.2.4. Non-linear regression and ANN

Non-linear relations between attributes and log properties restrict the ability of linear methods to estimate the parameters. Accordingly, non-linear methods, such as ANN, are used in order to estimate the reservoir parameters. The neural networks are mainly comprised of three layers: input, hidden, and output. Each layer in a network contains a collection of several units or neurons that are connected to each other according to some patterns. Such patterns facilitate the possibility of connection and transmission of data between the units. A weighted combination of these units will result in the output data. The ANNs are parallel calculating tools, which are comprised of many connected processors. Each processor in a network only deals with signals that receive and send to next processors alternatively. These locally simple processors, when placed in a rhythmical big network, find the capability of doing complex tasks.

Although various types of neural network algorithms exist, three types of neural networks are suitable to estimate the reservoir parameters: PNN, RBFN, and MLFN. In terms of geophysical and petrophysical properties, that is the main aim of this study, the seismic attributes and porosity logs are the inputs for the neural network and the effective porosity values are the optimum outputs (Edalat *et al.*, 2009). In practice, using the neural network for estimating porosity can be divided into four stages:

1. step-wise multi-linear regression analysis and its validation for recognising optimum number of attributes;
2. training neural networks to establish the non-linear relationship between seismic attributes and reservoir properties at well locations including validation and test;
3. apply trained neural networks to the seismic section;
4. validate results at well locations by dropping one well at a time and predicting it from other wells according to Basu and Verma (2013).

### 3.2.4.1. MLFN

Nowadays, the MLFN is perhaps the most popular network architecture in use (Panchal *et al.*, 2011). Multilayer neural networks are feed forward neural networks trained by the standard back propagation algorithm. Such networks are supervised networks and, therefore, they require a desired response for training. They learn how to transform input data into a desired response, accordingly, these networks are widely used for pattern classification. With one or two hidden layers, they can approximate virtually any input-output mapping. They are shown to approximate the performance of optimal statistical classifiers in difficult problems. Most neural network applications involve MLFNs (Panchal *et al.*, 2011).

### 3.2.4.2. PNN

The PNN is initially proposed by Specht (1990). This method is actually a mathematical interpolation scheme, which happens to use a neural network architecture for its implementation. The PNN assumes that each new output log value can be written as a linear combination of the log values as the training data. The biggest problem with the PNN is that, because it carries around all its training data and compares each output sample with each training sample, the application time can be slow (Hampson *et al.*, 2001). In PNN approach the weights are calculated using the concept of “distance” in attribute space from a known point to an unknown point. The basic idea behind PNN is to use a set of one or more measured values (independent variables) to predict the value of single dependent variable (Basu and Verma, 2013).

### 3.2.4.3. RBFN

The RBFN is a three-layer feed-forward network that uses a linear transfer function for the output units and a non-linear transfer function (normally the Gaussian) for the hidden layer neurons. Radial basis networks may require more neurons than standard feed-forward networks, but they can often be designed with less time. They perform well when many training data are available. Much of the inspiration for RBFN networks has come from traditional statistical pattern classification techniques.

## 4. Result and discussion

### 4.1. Estimation of acoustic impedance section

In this research, the Hampson-Russell software (1999) has been used for data interpretation. Data with the suitable format (seismic and well logging data with format of SEG-Y and LAS, respectively) are processed with the mentioned software. Then, by calibrating the well data to check-shot data, these data were transformed from depth to time in order to have both well-logging and seismic data in the time domain. In the next step, the exact locations of top and base of the Sarvak Formation were distinguished for the two wells. Thus, the Sarvak reservoir horizon was interpreted on this seismic line. The procedure, then, follows by wavelet extraction, synthetic seismogram production, and seismic-well tie. An acoustic impedance initial model was generated afterwards. Finally, the MBI was applied on the seismic section in order to extract the acoustic impedance from the seismic section. The input data for doing model-based seismic inversion is the seismic section with SEG-Y format, well logging data, which include P-wave velocity and

density logs with LAS format and check-shot data. Fig. 3 shows the acoustic impedance section at the two well locations that is obtained from model-based seismic inversion. This inverted section was used to estimate the porosity model of the area under study.

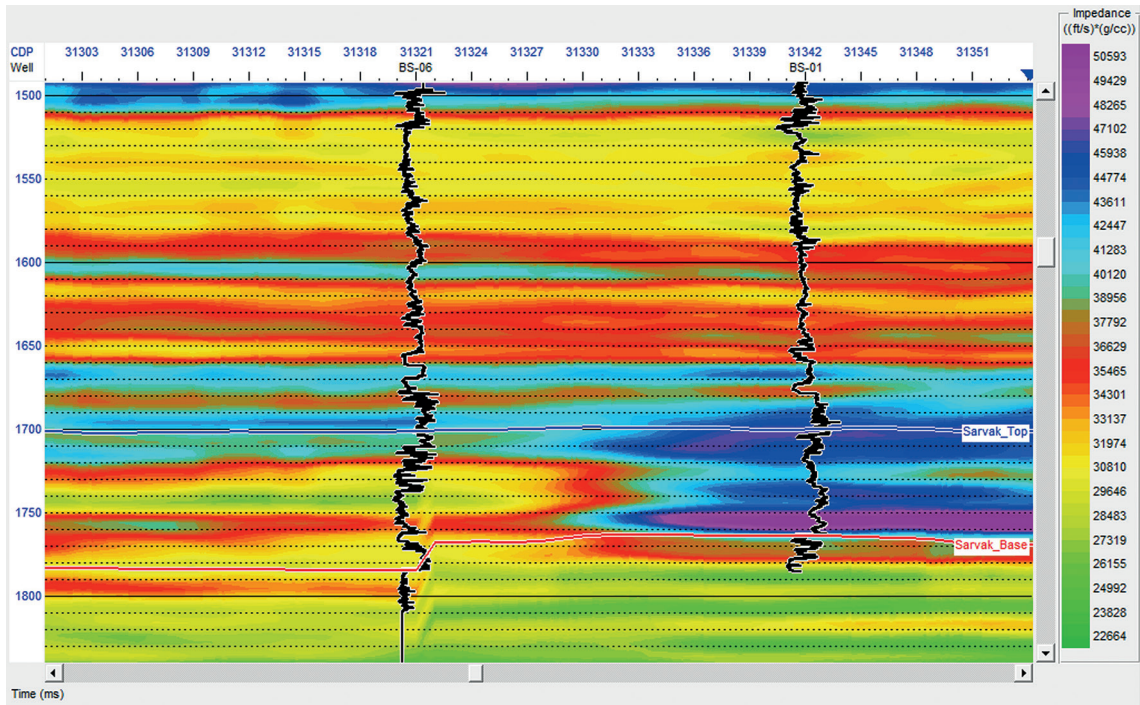


Fig. 3 - Acoustic impedance section derived from MBI at two well locations. The black well log curves are the sonic log. Blue and red horizons display Sarvak\_Top and Sarvak\_Base horizons, respectively. The X and Y axes are CDP locations and time, respectively. The colour key indicates the inverted acoustic impedance values.

#### 4.2. Estimation of porosity model

After extracting the acoustic impedance section, the porosity can be estimated using three methods: single-attribute regression, multi-attribute regression, and the PNN. In this process, seismic section, existing porosity logs at well locations, and the acoustic impedance section obtained from the model-based seismic inversion were used. These data were analysed by EMERGE module of the HRS. This module is used to merge well log and seismic data. The general objective is to predict a well log property using attributes of the seismic data. The seismic attributes may be calculated internally, or they may be provided as external attributes.

First, in order to determine the optimum single attribute, 160 samples on the seismic section were analysed. Table 1 shows the single attribute correlation results. The best attribute is the one with the highest correlation and the lowest prediction error (Hampson *et al.*, 2001). In this research it is found that the acoustic impedance resulted from the seismic inversion is the optimum single attribute. The error value and correlation coefficient between the estimated porosity log and the optimum single attribute was 80% and 6% (in percentage), respectively, as shown in Table 1. Note that the negative correlation coefficient is due to the fact that some attributes have a reverse relation with the estimated porosity. This means that an increase in the attribute will lead

to a decrease in porosity, i.e. the negative values still show correlation although in the reverse direction.

Table 1 - The single-attribute correlation results to determine the optimum single attribute. The target log is shown in the first column. The second column shows the optimum single attribute related to the target log. The third and fourth columns show the error value and correlation coefficient between the single attributes and the estimated porosity by these attributes (in percentage), respectively.

Target	Attribute	Error	Correlation
Porosity	Inversion Result	0.067467	-0.805131
Sqrt (Porosity)	(Inversion Result)**2	0.067547	-0.794621
Porosity	Sqrt (Inversion Result)	0.067695	-0.803653
Porosity	(Inversion Result)**2	0.067728	-0.803436
Porosity	Log (Inversion Result)	0.068153	-0.800651
Sqrt (Porosity)	Inversion Result	0.069267	-0.793625
Porosity	1/(Inversion Result)	0.069709	0.790233
Sqrt (Porosity)	Sqrt (Inversion Result)	0.070446	-0.790810
Sqrt (Porosity)	Log (Inversion Result)	0.071809	-0.786491
Log (Porosity)	(Inversion Result)**2	0.073043	-0.753388
Sqrt (Porosity)	1/(Inversion Result)	0.074989	0.773547
(Porosity)**2	1/(Inversion Result)	0.075185	0.781235
Log (Porosity)	Inversion Result	0.077514	-0.750157
There are 160 samples.			

Next, the estimation of porosity was carried out by using multi-attribute regression method. The previous researches showed that the set of attributes are sensitive to a reservoir properties and using multi-attribute regression can provide better results as compared to single-attribute regression method (Edalat *et al.*, 2009). In this method multiple secondary sets of seismic attributes were used. The optimum number of attributes was computed by using the step-wise regression and the cross-validation methods which was discussed in section 3.2.

The optimum composition of seismic attributes were first selected and, then, the porosity was estimated using the step-wise regression method with an operator length of three points. The Operator Length is the number of neighbouring points on each attribute, which are used to predict a single point on the target log. For example, if this is set to three, then each target log sample will be predicted using weighted values of three neighbouring samples on the attributes. The theoretical justification for this is that the seismic attributes are at a much lower frequency than the target logs, and they are in fact related to the logs by a convolutional operator (the wavelet). Note that as the operator length is increased, the RMS prediction error will always decrease, however, the danger of over-training is increased too. Also note that an operator length of one point is equivalent to conventional regression.

In this method, the best composition of existing attributes was determined according to the relation of each attribute with the target parameter and the existing error between them. The list of attributes determined by the step-wise regression algorithm along with their respective training and validation errors are shown in Table 2. This list shows the best fifteen attributes chosen by

the step-wise regression algorithm. Each row corresponds to a particular multi-attribute transform and includes all the attributes above it. For example, the first row, labelled “Inversion Result”, suggests that the best single attribute to use is the Inversion Result. The second row, “Apparent Polarity”, actually refers to a transform using both “Inversion Result” and “Apparent Polarity” simultaneously, and this is the best pair. As we proceed down the list, we get the best triplet, the best four, etc. The decreasing error shows that, as expected, the prediction error decreases with increasing the number of attributes.

Table 2 - List of attributes determined by step-wise regression algorithm. The target log is shown in the first column. The second column shows the best composition of existing attributes. Also, the third and fourth columns show the training error and validation error between the estimated target log and the real target log (in percentage), respectively.

	Target	Final Attribute	Training Error	Validation Error
1	Porosity	Inversion Result	0.066871	0.077794
2	Porosity	Apparent Polarity	0.059047	0.077351
3	Porosity	Filter 15/20-25/30	0.054685	0.074659
4	Porosity	Instantaneous Frequency	0.051140	0.073897
5	Porosity	Filter 25/30-35/40	0.047820	0.073527
6	Porosity	Second Derivative Instantaneous Amplitude	0.046644	0.087995
7	Porosity	Amplitude Weighted Phase	0.045594	0.090904
8	Porosity	Filter 45/50-55/60	0.043955	0.078358
9	Porosity	Second Derivative	0.042180	0.090035
10	Porosity	Filter 35/40-45/50	0.040113	0.096654
11	Porosity	Time	0.039156	0.139333
12	Porosity	Amplitude Envelope	0.038358	0.126451
13	Porosity	Amplitude Weighted Frequency	0.037017	0.114637
14	Porosity	Cosine Instantaneous Phase	0.035897	0.115334
15	Porosity	Filter 55/60-65/70	0.035375	0.100348

The cross-validation error helps to decide when too many attributes are included. Each point in the validation error is calculated by excluding each of the wells and predicting its values using the operator calculated by including other wells. Based on cross-validation error curve for porosity estimation shown in Fig. 4, it was observed that the validation error was reduced to only the first five numbers of seismic attributes (with two point convolution transform operator) and, then, it increases. Thus, the first five seismic attributes from Table 2 (including Inversion Result, Apparent Polarity, Filter 15/20-25/30, Instantaneous Frequency, and Filter 25/30-35/40) were selected for prediction of porosity section by multi-attribute regression method. Also, for estimation of porosity by using PNN method these five attributes were used.

Finally with the performance of multi-attribute regression on the seismic data, the porosity section of region is obtained. The cross-plot of the predicted porosity values versus true porosity values indicate that the amount of correlation between the estimated porosity log and the measured porosity log is 90% with 4% error, as shown in Fig. 5. Furthermore, the predicted porosity section by multi-attribute regression method at well locations BS-01 and BS-06 is depicted in Fig. 6.

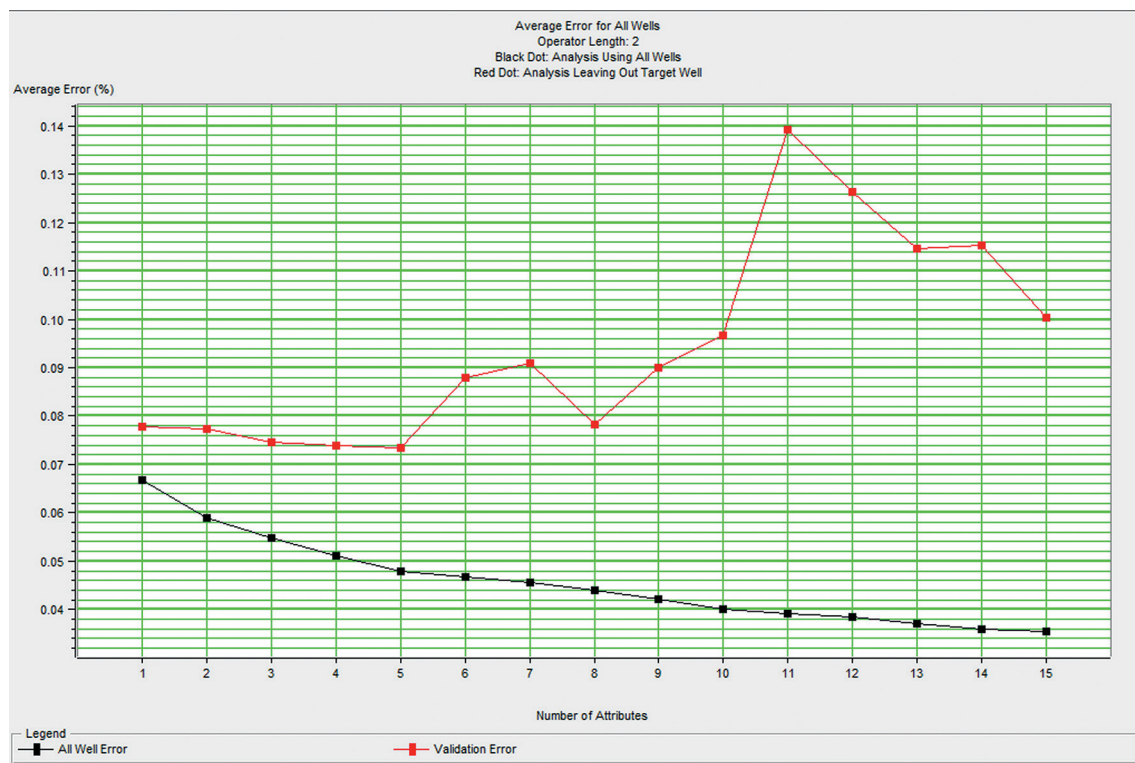


Fig. 4 - Graph of cross-validation error in multi-attribute method used for recognising optimum attributes numbers. The black (lower) curve shows the prediction error on the vertical axis and the number of attributes on the horizontal axis and the red (upper) curve is the validation error.

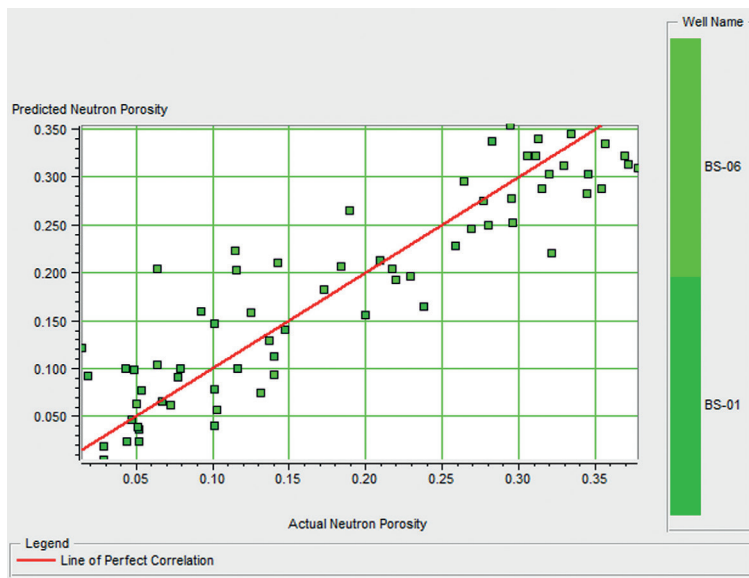


Fig. 5 - The cross-plot of predicted porosity versus measured porosity, for the two drilled wells. The X and Y axes are actual porosity at the two well locations and predicted porosity by using multi-attribute regression method, respectively. The actual correlation and error was 90% and 4%, respectively, that were calculated using 5 attributes and a 2-point convolutional operator.

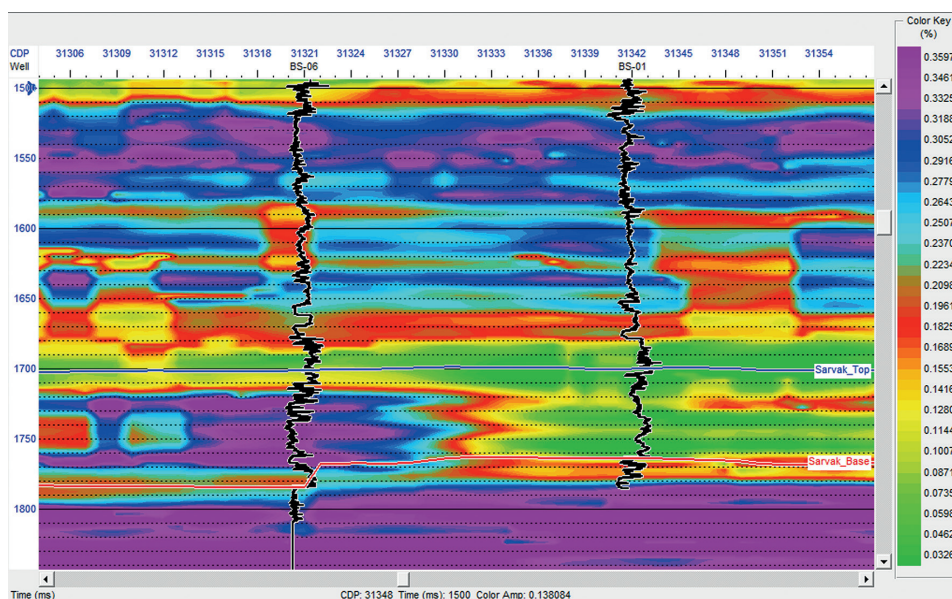


Fig. 6 - Predicted porosity section by multi-attribute regression method at location of the two wells. The black well log curves are the sonic log. The blue and red horizons display Sarvak\_Top and Sarvak\_Base horizons, respectively. The X and Y axes are CDP locations and time, respectively. The colour key indicates the predicted porosity values.

The final method used in this research is the neural networks. For this purpose, three different algorithms of the neural networks were trained and after validating the trained networks, the best network with high validation correlation values was selected for porosity estimation. The input data used in this step are the first five seismic attributes shown in Table 2 and the porosity logs at the two well locations. The porosity section is generated by applying the neural network on the inverted acoustic impedance section. For this purpose, the probabilistic, multilayer feed-forward, and the radial basic function neural network algorithms are used. The obtained values from these three methods are given in Table 3. In this research, the Intel Core i7 CPU, 2.70 GHz and the Intel® HD Graphics 3000 GPU, was used for computations. Regarding the obtained values, it is distinguished that the PNN with validation correlation of 78% and validation error of 7% presents superior and suitable results as compared to the two other networks. The results of applying the PNN on the inverted acoustic impedance section as the input to the network and the resultant porosity section is depicted in Fig. 7. Fig. 8 indicates that the highest reservoir quality takes place around the seismic CDP location No. 30850. It is located around 6 km far away from the two well positions. The BS-01 and BS-06 well distances from this CDP are 6552 and 6758 m, respectively.

Table 3 - Comparison between the obtained values from the three different ANN methods.

Neural Network Type	Correlation	Error	Validation Correlation	Validation Error	Computation Time
Probabilistic	94%	3%	78%	7%	40 min.
Multilayer Feed-Forward	99%	1%	58%	10%	28 min.
Radial Basis Function	96%	3%	0	11%	30 min.

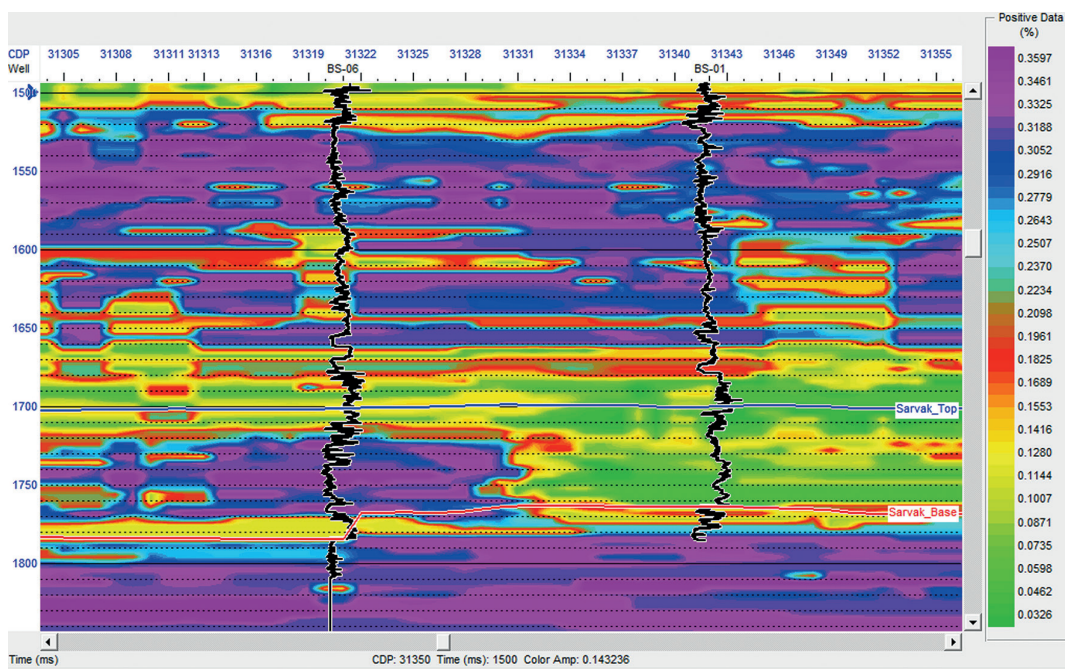


Fig. 7 - Predicted porosity section using PNN at BS-01 and BS-06 well locations. The black well log curves are the sonic log. Blue and red horizons display Sarvak\_Top and Sarvak\_Base horizons, respectively. The X and Y axes are CDP locations and time, respectively. The colour key indicates the predicted porosity values.

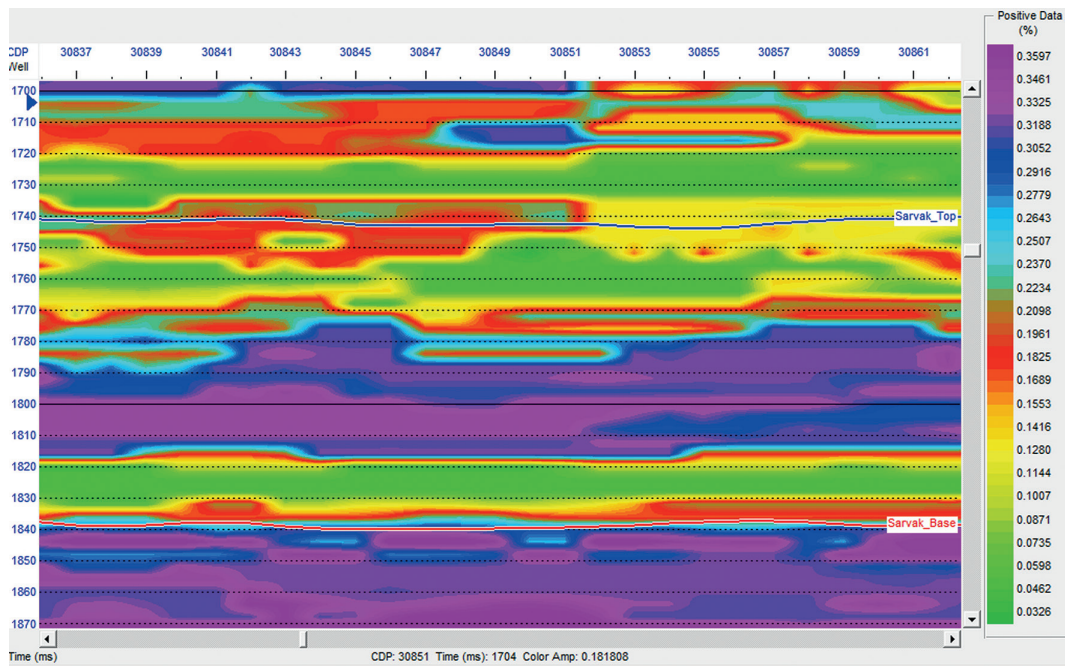


Fig. 8 - The highest porosity in the region related to CDP No. 30850. The X and Y axes are CDP locations and time, respectively. The colour key indicates the predicted porosity values.

### 4.2.1. Uncertainty analysis of the porosity section

In order to describe the numerical values obtained from the analysis with the respective uncertainties as well as uncertainty analysis of the porosity section, the PNN and multi-attribute methods are applied, the results obtained from the cross-plots are shown in Figs. 9 and 10. In these figures the cross-plot of porosity vs. acoustic impedance are displayed along with the error bars calculated for each sample related to both presented methods. For such purpose, a standard method is used in order to determine the prediction uncertainties, which is based on calculation of confidence intervals associated with the linear regressions obtained for each case (Ortet *et al.*, 2012). In these two figures, the linear regression line (solid line) along with upper and lower 95% confidence intervals (dashed line), obtained based on the standard deviation of the mean, are shown. Such depiction is an excessive illustration for the quality of the porosity/impedance models. As it is evident, the results from the multi-attributes method are better distributed within the confidence range.

Fig. 9 - The uncertainty analysis of predicted porosity using by the PNN method. The X and Y axes are acoustic impedance and porosity values, respectively. Also, the solid and dashed lines are linear regression and 95% confidence intervals, respectively.

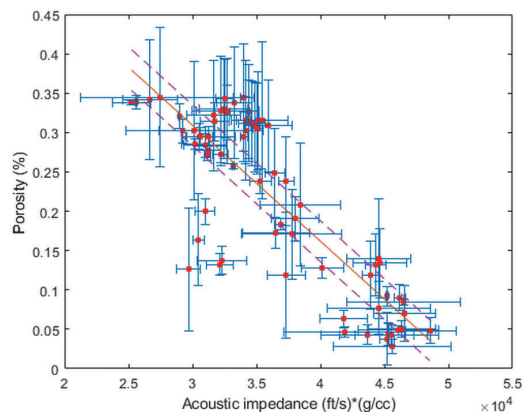
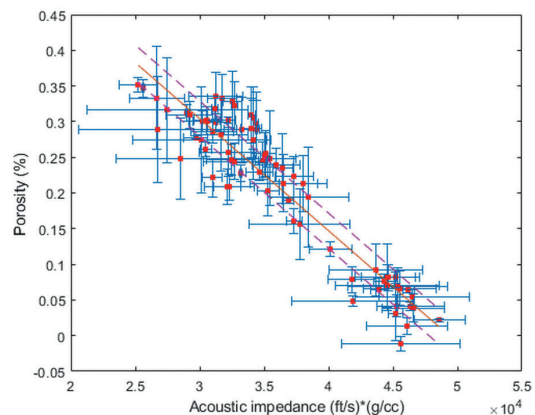


Fig. 10 - The uncertainty analysis of predicted porosity using by the multi-attributes method. The X and Y axes are acoustic impedance and porosity values, respectively. Also, the solid and dashed lines are linear regression and 95% confidence intervals, respectively.

The error bars and the upper and lower confidence intervals are shown for each sample based on the variance and the porosity distribution.

Finally, because the well logging data is more accurate than seismic data, it is suggested that more wells should be used to obtain more accurate results in similar studies. Furthermore, in order to obtain a higher resolution geological model, it is recommended that the three-dimensional (3D) seismic data should be used for similar analysis. Furthermore, the method used in this paper can be used to estimate fluid saturation and permeability models.

## 5. Conclusions

In this study, the porosity model of a reservoir layer in a hydrocarbon field located SW of Iran is estimated, using different types of available data (including seismic data, check shot data, and well logging data). We extract internal attributes and the acoustic impedance section as an external attribute from the seismic section. This research is based on predicting the reservoir porosity through various methods including single-attribute regression, multi-attribute regression, and PNN. First, the single-attribute was used for estimating reservoir porosity for which the result showed 80% correlation with 6% error between the estimated porosity log and the optimum single attribute (Table 1). In the next step, the estimation of porosity was done by using multi-attribute regression method for which the result showed 90% correlation with 4% error (Fig. 5) between estimated porosity log and the real porosity log. Finally, a PNN was trained using training and cross-validation data sets and it was used to predict the reservoir porosity model. The results showed a good correlation between real and predicted data, with 94% correlation and 3% error (Table 3). By single-attribute regression method, several attributes are selected and the porosity is estimated by performing multi-attribute transform on the inverted acoustic impedance section. Therefore, the best attributes are selected for porosity estimation using the multi-attribute regression method, using step-wise regression method, and investigating the validation error curvature. Then, using the selected list of seismic attributes and the porosity well logs, a PNN is designed and used for porosity estimation away from the wells. Accordingly, a continuous improvement in predictive power is observed as we progress from single-attribute regression to multi-attribute prediction and to PNN prediction. Moreover, this study shows the ability of the PNN networks to predict effective porosity even with a paucity of training exemplars. Furthermore, studying the obtained porosity model, it is recognised that the highest value of porosity in the region is related to the seismic CDP location No. 30850, which can be recommended for future drilling. The outcome of his study may be used as a guide for further development of the area.

**Acknowledgements.** The second author would like to acknowledge Research Council of the University of Tehran. Thanks are given to anonymous domain experts for their input and insight without which this research would not have been possible. This research did not receive any specific grant from funding agencies in the public, commercial, or not-for-profit sectors.

## REFERENCES

- Al-Rahim A.M. and Hashem H.A.; 2016: *Subsurface 3D prediction porosity model from converted seismic and well data using model based inversion technique*. Iraqi J. Sci., **57**, 163-174.
- Basu P. and Verma R.; 2013: *Multiattribute transform and probabilistic neural network in effective porosity - A case study from Nardipur low area, Cambay Basin, India*. In: Proc., 10th Biennial International Conference & Exposition, Society of Petroleum Geophysicists, Kochi, India, P131, 8 pp.
- Behdad A., Vaziri-Moghaddam H., Taheri A. and Taati F.; 2010: *Microfacies and depositional environment of the Cenomanian of the Bangestan anticline, SW Iran*. J. Asian Earth Sci., **37**, 275-285, doi: 10.1016/j.jseas.2009.08.014.
- Beiranvand B., Ahmadi A. and Sharafodin M.; 2007: *Mapping and classifying flow units in the upper part of the mid-Cretaceous Sarvak Formation (western Dezful Embayment, SW Iran) based on a determination of the reservoir types*. J. Petrol. Geol., **30**, 357-373, doi: 10.1111/j.1747-5457.2007.00357.x.
- Çemen I., Fuchs J., Coffey B., Gertson R. and Hager C.; 2014: *Correlating porosity with acoustic impedance in sandstone gas reservoirs: examples from the Atokan sandstones of the Arkoma Basin, southeastern Oklahoma*. In: Proc., Annual Convention Exhibition, Search and Discovery, American Association Petroleum Geologists, Pittsburgh, PA, USA, Article #41255.
- Central Intelligence Agency; 2001: *Geographic position of some hydrocarbon fields in the Persian Gulf*. Washington, DC, USA.
- Dolberg D.M., Helgesen J., Hanssen T.H., Magnus I., Saigal G. and Pedersen B.K.; 2000: *Porosity prediction from seismic inversion, Lavrans Field, Halten Terrace, Norway*. The Leading Edge, **19**, 392-399, doi: 10.1190/1.1438618.

- Edalat A., Siyahkuhi H.R. and Tavakkoli Moghaddam R.; 2009: *Estimation of effective porosity by using Multi-attribute analysis*. J. Iran. Geophys., **3**, 1-18.
- Hajikazemi E., Al-Aasm I. and Coniglio M.; 2010: *Subaerial exposure and meteoric diagenesis of the Cenomanian-Turonian upper Sarvak Formation, southwestern Iran*. In: Tectonic and Stratigraphic Evolution of Zagros and Makran during the Mesozoic–Cenozoic, Geological Society London, Special Publications, vol. 330, pp. 253-272, doi: 10.1144/SP330.12.
- Hajikazemi E., Al-Aasm I. and Coniglio M.; 2012: *Chemostratigraphy of Cenomanian-Turonian carbonates of the Sarvak Formation, southern Iran*. J. Petrol. Geol., **35**, 187-206, doi: 10.1111/j.1747-5457.2012.00525.x.
- Hampson D.P., Schuelke J.S. and Quirein J.A.; 2001: *Use of multiattribute transforms to predict log properties from seismic data*. J. Geophys., **66**, 220-236, doi: 10.1190/1.1444899.
- Hampson-Russell software; 1999: *Theory of the Strata program*. Hampson-Russell Software Services Ltd, Calgary, Canada, 64 pp., <www.cgg.com/data/1/rec\_docs/585\_STRATA\_Theory.pdf>.
- Haykin S.; 1999: *Neural networks: a comprehensive foundation, 2<sup>nd</sup> ed.* Prentice Hall, Upper Saddle River, NJ, USA, 842 pp.
- Leiphart D.J. and Hart B.S.; 2001: *Comparison of linear regression and a probabilistic neural network to predict porosity from 3D seismic attributes in lower Brushy Canyon channeled sandstones, southeast New Mexico*. J. Geophys., **66**, 1349-1358.
- Li M. and Zhao Y.; 2014: *Prestack seismic inversion and seismic attribute analysis*. In: Geophysical Exploration Technology, Applications in Lithological and Stratigraphic Reservoirs, Elsevier Inc., Amsterdam, The Netherlands, Chapter 7, pp. 199-219, doi: 10.1016/B978-0-12-410436-5.00007-1.
- Mahmood M.F., Shakir U., Abuzar M.Kh., Ali-Khan M., Khattak N., Hussain H.Sh. and Tahir A.R.; 2017: *Probabilistic neural network approach for porosity prediction in Balkassar area: a case study*. J. Himalayan Earth Sci., **50**, 111-120.
- Maurya S.P. and Singh K.H.; 2019: *Predicting porosity by multivariate regression and probabilistic neural network using model-based and coloured inversion as external attributes: a quantitative comparison*. J. Geol. Soc. India, **93**, 207-212, doi: 10.1007/s12594-019-1153-5.
- McKie T., Rose P.T.S., Hartley A.J., Jones D.W. and Armstrong T.L.; 2015: *Tertiary deep-marine reservoirs of the North Sea region: an introduction*. In: McKie T., Rose P.T.S., Hartley A.J., Jones D.W. and Armstrong T.L. (eds), Tertiary Deep-Marine Reservoirs of the North Sea Region, 1 ed., Geological Society of London, England, Special Publications, Vol. 403, pp. 1-16, doi: 10.1144/SP403.12.
- Omidvar M., Mehrabi H. and Sajjadi F.; 2015: *Depositional environment and biostratigraphy of the upper Sarvak Formation in Ahwaz oilfield (well No. 63)*. Sediment. Facies, **7**, 158-177, doi: 10.22067/sed.facies.v7i2.23441.
- Ortet S., Vidal O., Fournier F., Guillemot D., Hayet M. and Yven B.; 2012: *Estimation of uncertainties associated to porosity prediction from inversion*. In: Proc., 82<sup>nd</sup> Annual Meeting, Society of Exploration Geophysicists, Las Vegas, NV, USA, 5 pp.
- Panchal G., Ganatra A., Kosta Y.P. and Panchal D.; 2011: *Behaviour analysis of multilayer perceptrons with multiple hidden neurons and hidden layers*. Int. J. Comput. Theory Eng., **3**, 332-337, doi: 10.7763/IJCTE.2011.V3.328.
- Parsaeimaram M., Rao K.M.R. and Poursalehi A.; 2013: *An artificial neural network for prediction of seismic behavior in RC buildings with and without infill walls*. Int. J. Mod. Eng. Res., **3**, 3071-3078.
- Rahimpour-Bonab H.; 2007: *A procedure for appraisal of hydrocarbon reservoir continuity and quantification of its heterogeneity*. J. Pet. Sci. Eng., **58**, 1-12, doi: 10.1016/j.petrol.2006.11.004.
- Rahimpour-Bonab H., Mehrabi H., Enayati-Bidgoli A. and Omidvar M.; 2012a: *Coupled imprints of tropical climate and recurring emergence on reservoir evolution of a mid Cretaceous carbonate ramp, Zagros Basin, southwest Iran*. Cretaceous Res., **37**, 15-34, doi: 10.1016/j.cretres.2012.02.012.
- Rahimpour-Bonab H., Mehrabi H., Navidtalab A. and Izadi-Mazidi E.; 2012b: *Flow unit distribution and reservoir modeling in Cretaceous carbonates of the Sarvak Formation, Abteymour oilfield, Dezful Embayment, SW Iran*. J. Pet. Geol., **35**, 213-236, doi: 10.1111/j.1747-5457.2012.00527.x.
- Russell B.H.; 2004: *The application of multivariate statistics and neural networks to the prediction of reservoir parameters using seismic attributes*. PH.D. Thesis in partial fulfilment of the requirements for the degree of Doctor of Philosophy, Department of Geology and Geophysics, University of Calgary, Calgary, AB, Canada, 392 pp.
- Specht D.F.; 1990: *Probabilistic neural networks*. Neural Networks, **3**, 109-118.
- Taghavi A., Mork A. and Emadi M.; 2006: *Sequence stratigraphically controlled diagenesis governs reservoir quality in the carbonate Dehloran field, southwest Iran*. Pet. Geosci., **12**, 115-126, doi: 10.1144/1354-079305-672.
- Taner M.T.; 2001: *Seismic attributes*. Can. Soc. Explor. Geophys. Rec., **26**, 48-56.
- Varasteh A., Siyahkuhi H.R., Khamechi A. and Norouzi S.; 2010: *Application of seismic coherence attributes in describing the reservoir's faults and fractures*. J. Petrol. Res., **22**, 64-72.

Corresponding author: Mohammad Ali Riahi  
 Institute of Geophysics, University of Tehran  
 North Kargar Ave., Tehran, Iran  
 Phone: +98 21 61118219; e-mail: mariahi@ut.ac.ir